Factors Affecting Perceptual Thresholds in a Suprachoroidal Retinal Prosthesis

Mohit N Shivdasani[1,3,*], Nicholas C Sinclair[1], Peter N Dimitrov[2], Mary Varsamidis[2], Lauren N Ayton[2], Chi D Luu[2], Thushara Perera[1], Hugh J McDermott[1,3], and Peter J Blamey[1,3] for the Bionic Vision Australia Consortium[#]

#The Bionic Vision Australia Consortium consists of five member organizations (Centre for Eye Research Australia, Bionics Institute, NICTA, University of Melbourne and University of New South Wales) and three partner organizations (The Royal Victorian Eye and Ear Hospital, National Vision Research Institute of Australia and the University of Western Sydney). For this publication, the consortium members consist of (in alphabetical order): Penelope J Allen[2], Tamara-Leigh E Brawn[5], Robert Briggs[2], Anthony N Burkitt[5], Owen Burns[1], James B Fallon[1], Lisa Gillespie[1], Robyn H Guymer[2], Wilson Heriot[2], Nigel H Lovell[4], Mark McCombe[2], Michelle McPhedran[1], Rodney Millard[1], David AX Nayagam[1], Nicholas L Opie[2], Matthew A Petoe[1], Alexia Saunders[1], Peter M Seligman[1], Kyle Slater[1], Robert K Shepherd[1,3], Gregg J Suaning[4], Joel Villalobos[1], Chris E Williams[1,3] and Jonathan Yeoh[2].

[1]Bionics Institute, East Melbourne, AUSTRALIA

[2]Centre for Eye Research, The University of Melbourne, Royal Victorian Eye & Ear Hospital, East Melbourne, AUSTRALIA

[3]Department of Medical Bionics, The University of Melbourne, AUSTRALIA

[4]Department of Biomedical Engineering, University of New South Wales, AUSTRALIA

[5]Bionic Vision Australia, Carlton, Victoria, AUSTRALIA

*Corresponding Author:

Dr. Mohit N. Shivdasani

Bionics Institute, 384-388 Albert Street, East Melbourne, VIC – 3002, AUSTRALIA

Email: mshivdasani@bionicsinstitute.org

Word Count: 8490

Grant Information:

This work was supported by the Australian Research Council through its Special Research Initiative in Bionic Vision Science and Technology awarded to Bionic Vision Australia and by the Bertalli Family Foundation to the Bionics Institute. The Bionics Institute and the Centre for Eye Research Australia (CERA) acknowledge the support received from the Victorian Government through its Operational Infrastructure Program. CERA is also supported by an NHMRC Centre for Clinical Research Excellence Award #529923.

Abstract

Purpose: The suprachoroidal location for a retinal prosthesis provides advantages over other locations in terms of a simplified surgical procedure and a potentially more stable electrode-neural interface. The aim of this study was to assess the factors affecting perceptual thresholds, and to optimize stimulus parameters to achieve the lowest thresholds in patients implanted with a suprachoroidal retinal prosthesis.

Methods: Three patients with profound vision loss from retinitis pigmentosa were implanted with a suprachoroidal array. Perceptual thresholds measured on individual electrodes were analyzed as a function of stimulus (return configuration, pulse polarity, pulse width, interphase gap and rate), electrode (area and number of ganged electrodes), and clinical (retinal thickness and electrode-retina distance) parameters.

Results: A total of 92.8% of 904 measurements made up to 680 days post-implantation, yielded thresholds (Range 44-436nC) below the safe charge limit. Thresholds were found to vary between individuals and depend significantly on electrode-retina distance, negligibly on retinal thickness, but not on electrode area, or the number of ganged electrodes. Lowest thresholds were achieved when using a monopolar return; anodic-first polarity; short pulse widths (100µs) combined with long interphase gaps (500µs); and high stimulation rates (≥400pps).

Conclusions: With suprachoroidal stimulation, anodic first pulses with a monopolar return are most efficacious. To enable high rates, an appropriate combination of pulse width and interphase gap must be chosen to ensure low thresholds and electrode voltages. Electrode-retina distance needs to be monitored carefully owing to its influence on thresholds. These results inform implantable stimulator specifications for a suprachoroidal retinal prosthesis.

Introduction

Since the research efforts of Brindley and Lewin in the 1960s to restore vision through electrical stimulation of the visual cortex[1, 2], significant advances have been made in the development of a retinal prosthesis for vision restoration in patients with retinal degeneration. Retinal prostheses work via electrical stimulation of the surviving neurons and have been approved by the Food and Drug Administration (USA) and the European Commission (European Economic Area) as a safe and effective treatment for those suffering from degenerative retinal disorders such as retinitis pigmentosa (RP). There are two devices which have proceeded to commercialization, one being the Argus II™ from Second Sight Medical Products (Sylmar, CA, USA), which has both CE approval in Europe, and FDA approval in the United States[3], and the other being the Alpha IMS™ implant from Retina Implant AG (Reutlingen, Germany)[4], which recently gained CE approval in Europe[3]. These devices differ significantly in almost all aspects, but particularly in the location of implantation (epiretinal versus subretinal), the number of stimulating electrodes (60 versus 1500) and the technology used for image capturing (camera versus photodiode array). Although fundamentally different in their technology, both devices have proven their effectiveness through multi-center long term clinical trials[4, 5], with several implantees being able to recognize and discriminate objects[4, 6], detect motion[5, 7], and discriminate patterns to a fairly reasonable degree[4, 5, 8]. Some patients are even able to use the devices to navigate independently[4, 9], read large print[4, 10] and perform tasks involving activities of daily living[4], which is a testament to the usefulness of the technology.

Despite the positive outcomes with the present devices, there have been reports of several clinical complications found during clinical trials, including conjunctival erosion, hypotony, retinal detachment, endophthalmitis in patients with epiretinal devices[5], and a sustained increase in the number of microaneurysms in patients with subretinal devices[11]. Moreover,

the surgical procedures to implant these devices require multiple manipulations to the eye before the intraocular device is implanted, for example a pars-plana vitrectomy for both epiretinal[12] and subretinal approaches[13], and an obligatory cataract operation[14] and creation of a retinal bleb[13] with the subretinal approach. Finally, long-term device stability may become an issue with the use of retinal tacks for the epiretinal approach. Despite this safety profile, these devices have been approved by regulatory agencies with the benefits currently outweighing the risks, and are commercially available for implantation. In order to alleviate some of the complications and significantly simplify the surgical procedure, our group has been developing a suprachoroidal approach whereby the electrode array component of the prosthesis is inserted into the space between the sclera and choroid[15, 16]. The most significant advantage of this surgical approach is that the electrode array is held stable within the natural cleavage plane of the suprachoroidal space, thus eliminating the need for external elements such as retinal tacks to fixate the device to the retina. Moreover, the surgery only requires one layer of the eye (the sclera) to be breached for insertion of the electrode array[15], thus making it less invasive and reducing the risks of adverse events compared to the other approaches.

It is thought that while the suprachoroidal location may provide a more stable electrode-tissue interface, significantly higher levels of charge will be necessary to elicit visual percepts, owing to the greater distance between the electrode array and the target retinal ganglion cells (RGCs), compared to epiretinal and subretinal placements[17]. The increased charge may further result in unwanted current spread leading to decreased resolution, and may ultimately affect visual acuity and performance outcomes. This hypothesis has in part been corroborated by a small clinical trial conducted by a research group in Japan[18]. In their study, electrodes were placed within an intra-scleral pocket of two RP patients, and it was reported that considerably higher charge levels were required to reach perceptual threshold compared to those previously reported in epiretinal studies[19]. However, due to the short term of

implantation in that study (four weeks), it was not possible to test the effects of varying stimulus parameters on thresholds, and therefore all parameters were kept fixed at a "best guess" estimate based on their previous preclinical work[18]. For example, it is well known with both cochlear[20] and retinal implants[21] that high rates of stimulation result in lower perceptual thresholds than low rates – this was not explored in their study. The Second Sight group investigated the effects of varying stimulus parameters on thresholds with the Argus I device[21], while all threshold measurements with the Argus II device were made using a fixed set of parameters[19]. Thus there is a lack of longitudinal data regarding the effects of stimulus parameters and other factors on perceptual thresholds.

Through numerous preclinical studies[16, 22-25], our group validated the safety and efficacy of suprachoroidal stimulation which led to commencement of a phase 1 clinical trial (www.clinicaltrials.gov, trial #NCT01603576) in three RP patients in 2012[17, 26, 27]. Since then, we have monitored perceptual thresholds over nearly 24 months, and have therefore had more time to assess the effects of varying stimulus parameters. The main goals of this study were to: provide further evidence of successful stimulation of the retina via an electrode array placed in the suprachoroidal space of blind humans with advanced RP; assess thresholds required to elicit phosphene percepts; assess which stimulus parameters affect thresholds the most; and provide insights on what combination of parameters are ideal in order to obtain the lowest perceptual thresholds.

Materials and Methods

Patient Selection and Device Description

The research followed the tenets of the Declaration of Helsinki and informed consent was obtained from all participants upon explanation of the nature and possible consequences of the study. All procedures were approved by the Human Research Ethics committee of the Royal Victorian Eye and Ear Hospital and the clinical trial was registered at www.clinicaltrials.gov (trial #NCT01603576). Three patients with end-stage RP (one 53-year old female [P1], and two males aged 50 [P2] and 63 years [P3], were selected for implantation after a comprehensive screening process involving 95 people with RP. All patients had between 8-10 years (P2) and 20 years (P1 and P3) of light perception only vision. The worse-seeing eye was selected for implantation, and had bare light perception acuity in all three patients. This was determined during three separate pre-operative clinical assessments, which included a range of tests such as visual acuity, electroretinography and perimetry[28]. Between May and August 2012, all patients were implanted with a prototype suprachoroidal retinal prosthesis developed by the Bionics Institute through Bionic Vision Australia. The prosthesis consisted of an intraocular electrode array made of medical grade silicone (19 x 8mm), containing 35 platinum disk electrodes (Fig. 1A; 3 x 400µm diameter, 30 x 600µm diameter and 2 x 2000µm diameter). The electrodes on the top, bottom and leadwire ends of the array were shorted together to form a “guard ring” return electrode (Fig. 1B). The largest diameter electrodes were placed at the leadwire end of the array and acted as additional return electrodes (Fig. 1A). A platinum pin implanted subcutaneously behind the ear served as the fourth extraocular return electrode (Fig. 1C). Thus there were 20 stimulating electrodes and 4 choices of return electrodes. Each electrode was attached to a single 20µm

diameter platinum-iridium wire. The helically coiled leadwire (150mm long, 1.5mm diameter) exited the eye and connected the electrode array to a titanium percutaneous plug that exited the skin behind the ear (Fig. 1C). The use of a percutaneous plug enabled direct access to the electrodes via an external stimulator, thus eliminating the need for implantable electronics and providing maximum flexibility in the use of different electrode configurations

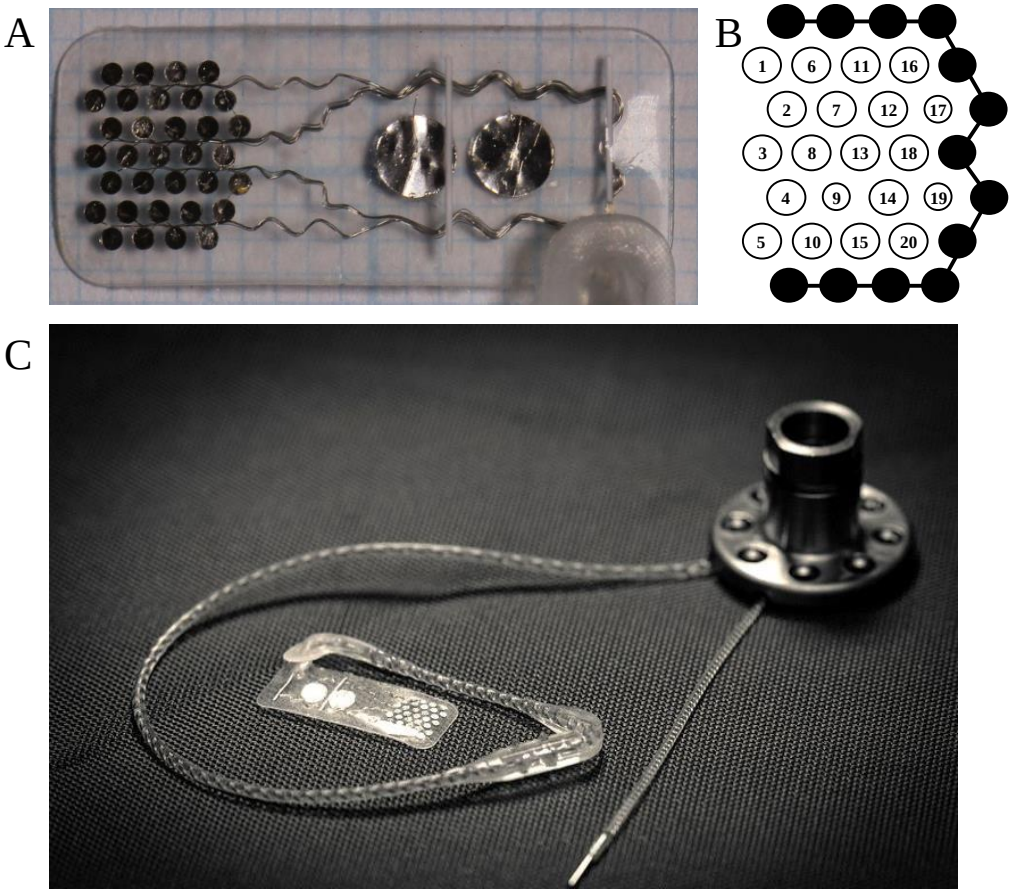

and parameters for stimulation.

Figure 1. The prototype suprachoroidal retinal prosthesis. (A) Intraocular silicone electrode array with 33 platinum disk electrodes (all disks were the same size but varied in exposed area of platinum: 3 x 400µm diameter and 30 x 600µm diameter stimulating electrodes) and 2 x 2000µm diameter return electrodes. (B) Electrode numbering scheme. Note: electrodes filled in black were shorted together to form the "guard ring" return (electrode 21), and electrodes 9, 17 and 19 were smaller in exposed area. (C) The full prosthesis with

intraocular array, helical leadwire, extraocular platinum pin return electrode, and titanium percutaneous plug. Photos provided by David AX Nayagam.

Surgical Procedure

The surgical procedures were similar to those performed in preclinical studies both in felines[16] (intraocular component only) and in cadaver humans[15]. Briefly, a curved incision was made behind the ear through the posterior temporalis muscle to expose a flat section of temporal bone. A tunnel was created beneath the temporalis fascia up to the orbital rim. After performing a lateral canthotomy, disinserting the lateral rectus muscle, and making the required scleral incision, the device was tunneled from behind the ear using a custom trocar up to the lateral orbital margin. The percutaneous plug was secured to the temporal bone with self-tapping screws. A pocket was made within the suprachoroidal space using a lens glide and the electrode array was inserted. A lateral orbitomy was created using 10mm burrs to stabilize the lead. Upon closure of the scleral wound through suturing of a Dacron patch, stabilization of the leadwire, and re-attachment of the lateral rectus muscle, an indirect ophthalmoscope was used to check the position of the electrode array in relation to the optic disk and the macula. An electrode connectivity test was performed immediately after surgery to confirm that all wires/electrodes were intact by passing a small test biphasic current pulse (75μA, 25μs per phase) and measuring the electrode voltage. Patients remained in hospital for 4-5 days post surgery and were given topical steroids, antibiotic eye drops and systemic analgesia as required. More details regarding the surgical procedures will be the subject of another manuscript.

Clinical and Psychophysical Sessions

Upon discharge from the hospital, patients underwent clinical assessment every week, where images were taken using color fundus photography (TRC-50Dx, Topcon Medical Systems, NJ) and spectral-domain optical coherence tomography (OCT; Spectralis, Heidelberg Engineering GmbH, Heidelberg, Germany). Using the images from the weekly OCT scans, retinal thickness as well as the distance between individual electrodes on the array and the retina (taken from the anterior surface of each disk to the retinal pigment epithelium) were measured (Fig. 2). In addition, the percutaneous plug and wound were closely examined and cleaned as necessary, and intra-ocular pressure measurements were made using contact tonometry (TonoPen XL, Reichert Technologies, Depew, NY). Post-surgical follow-ups were completed on a monthly basis to check ocular health, X-ray images were taken monthly for the first six months and at 12 months, and a full-head computed tomography scan was performed at 1 month and 12 months.

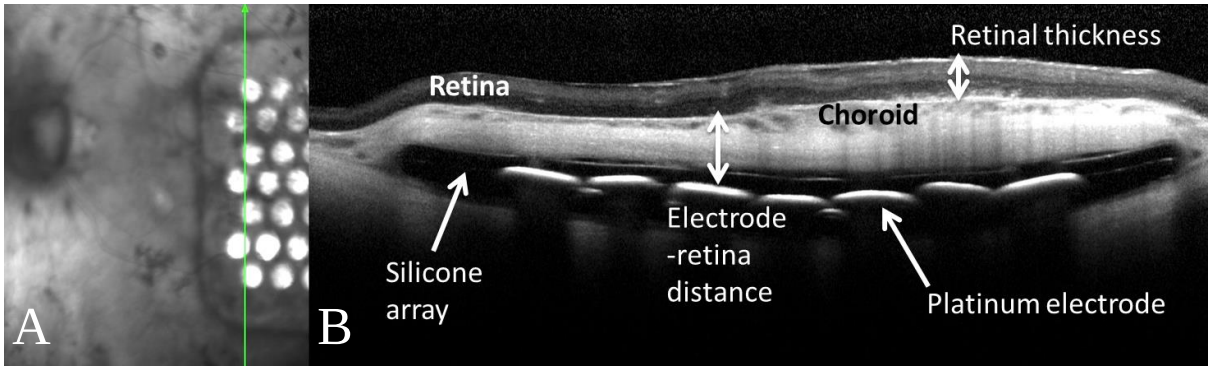

Figure 2. OCT scan of the electrode array in situ. The vertical arrow on the infrared image (A) indicates the direction of the OCT scan. The cross-sectional OCT image (B) shows the, the retina and choroid, silicone and platinum electrodes and the methods for determining retinal thickness and electrode-retina distance.

All patients experienced a combined suprachoroidal and subretinal hemorrhage post surgery, which resolved without a need for intervention in all cases (Fig. 3). The extent of the hemorrhage was limited to the area covered by the electrode array. In P2, a fibrotic tissue reaction occurred most likely due to hemorrhage at the temporal end of the implant and remained following hemorrhage resolution, but this should not have affected device efficacy and did not cause complications such as retinal detachment. P1 and P3 commenced weekly psychophysics sessions of 2-4 hours at the Bionics Institute between 1 and 2 months post-implantation. Sessions with P2 commenced approximately 3 months post-implantation, due to a slower post-surgical recovery. While it was possible to start psychophysical testing much earlier, the subretinal and suprachoroidal hemorrhage was not something we experienced in preclinical studies and it was the first time that electrodes had been inserted into the suprachoroidal space of blind humans. Whilst Fujikado et al[18] also described their technique as suprachoroidal, since their electrodes were in fact intra-scleral and not in direct contact with the choroid, this may explain why they did not report any hemorrhage. The hemorrhage seen in our study also impeded the visualization of electrodes under OCT. Therefore, as a precaution it was deemed by the clinical team to begin testing only once the hemorrhage had cleared.

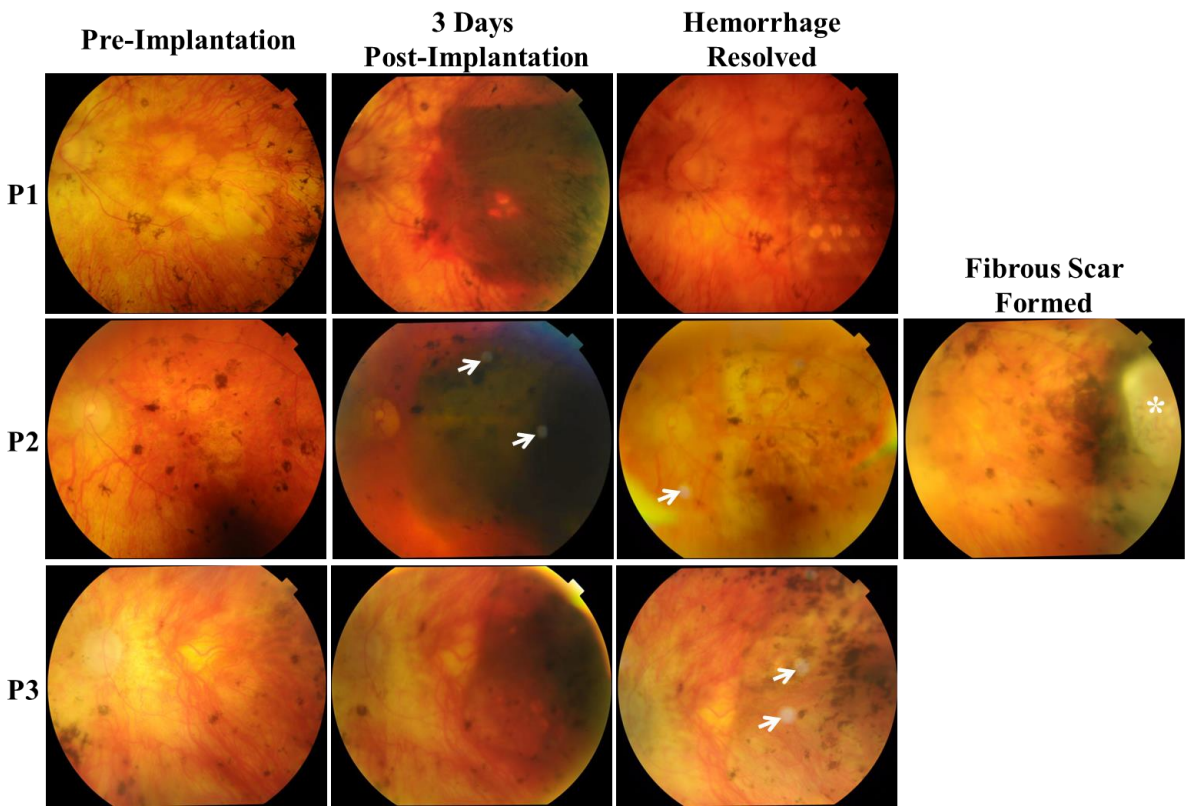

Figure 3. Color fundus images for all three patients at pre-implantation, at detection of hemorrhage post-implantation and at resolution of hemorrhage. White arrows in P2 and P3 indicate lens reflection artifacts. In P2, once the hemorrhage was resolved, a fibrous scar (*) was detected at the temporal end of the array which should not have affected any device efficacy.

At each psychophysics session, the patient was connected to an in-house designed and manufactured external bench-top stimulator (neuroBi™) using a custom flexible cable. The neuroBi™ stimulator is completely electrically isolated via a USB connection to a laptop computer and consists of a single current source. The current source is routed through a multiplexer to allow flexible stimulation of any single or ganged combination of electrodes on the array. The stimulator is capable of delivering charge-balanced symmetric biphasic pulses using currents up to 10mA, and pulse widths ranging from 20 to 3000µs per phase, at

frequencies of up to 6,250 pulses per second (pps), within a 40V voltage compliance. To ensure that overstimulation above safe charge and charge density levels were not performed, the charge on each electrode was capped to 447nC and 298nC (equating to an upper limit of charge density of 158μC/cm^2 and 237μC/cm^2), for the 600μm and 400μm diameter electrodes respectively. This charge limit was based on the data presented in Merrill et al.[29], and calculated using the well-accepted Shannon equation[30], with a conservative value of k=1.85. In addition to being connected to the stimulator, the patient also wore a pair of glasses that contained an eye tracker (Arrington Research Inc., AZ) and head motion detection system (Ascension Technology Corp, VT). Finally, to avoid any static discharge, the patient and the operator wore elastic wrist bands that were grounded to static shielded floor mats, which were in turn connected to earth. More details regarding the flexible psychophysics system will be the subject of another manuscript.

Threshold Measurement Technique

The threshold measurement technique was based on a well-established adaptive up-down staircase procedure that has been used extensively for psychophysics[31]. The procedure involved presenting multiple trials and detecting turning points (Fig. 4). For any given threshold measurement, the electrode being stimulated, return configuration, pulse polarity, pulse width, interphase gap, stimulation rate and duration of each trial were kept constant with only the charge per phase allowed to vary. The threshold procedure began with selecting an initial value of charge (100nC by default) to be delivered. Each trial was a train of biphasic pulses with a total duration of two seconds. The duration between trials was kept to approximately 3 seconds.

Patients were told when the threshold procedure began and were asked to respond “yes” whenever they saw a phosphene. However, with the exception of P3 (details below), patients

were not told explicitly when each trial exactly began within the procedure. Upon presentation of each trial, the operator would pause for approximately 3 seconds and if there was no response from the patient, the operator would enter a “no” response. Each “yes” or “no” response automatically determined a charge per phase to be delivered for the next trial. During the “up” phase, the charge per phase was increased until a “yes” response was encountered. The next trial following the first “yes” response during the “up” phase was presented using the same charge per phase as the previous trial. If two consecutive “yes” responses were encountered, the “down” phase of the procedure began where the charge per phase was decreased until a “no” response was encountered. Turning points were defined as either the second of two consecutive trials with “yes” responses using the same charge per phase during the “up” phase, or the first trial at which a “no” was encountered during the “down” phase. The step size used to increase or decrease the charge was 1dB (approximately 12%) until the first turning point, and 0.33dB (approximately 4%) thereafter. The procedure was completed and deemed successful after 8 turning points were detected and the final threshold value was recorded as the average charge per phase delivered in the last 6 turning points. If the charge per phase to be delivered reached the defined safe charge limit before achieving 8 turning points, then the procedure was aborted and it was recorded that no threshold was obtainable for that combination of electrode and stimulus parameters. Each threshold measurement on average, took approximately 5-6 minutes but could sometimes take longer (up to 10 mins). The procedure proved to be very reliable in determining a threshold, which could subsequently be confirmed by presenting a stimulus at threshold and getting a “yes” response and presenting a slightly sub-threshold stimulus and getting a “no” response. Also, both P1 and P2 gave consistent responses (i.e. perception or no perception agreed with stimulus strength), and false positives were not explicitly measured. This was not the case however, for P3 where it was necessary to explicitly test for false positives.

For P3, at the first few sessions, the standard threshold procedure was used. This procedure turned out to be very difficult for the patient, and often resulted in false positives and negatives. It was learnt later that the patient was seeing spontaneous phosphenes during the procedure that occurred independent of electrical stimulation, and were the reason for the false positives and negatives. Due to these difficulties, the threshold procedure was altered for P3 to a three-alternative forced choice protocol. This was similar to the standard procedure with the exception that each trial consisted of three pulse train presentations (each 2 secs) separated by 0.5s intervals. Two randomly selected pulse trains were delivered using zero charge per phase and the remaining pulse train was presented with the desired charge per phase. Each pulse train also coincided with an audio tone so the patient would hear 3 beeps on each trial and was able to identify which presentation elicited a phosphene when the charge per phase delivered was at or above perceptual threshold. This procedure turned out to be much more reliable for the patient and allowed valid thresholds to be measured along with accurate detection of false positives.

Figure 4. An example of the up-down staircase procedure used for threshold measurements. Each trial consisted of a pulse train lasting 2 secs. The subject was asked to verbally respond

"Yes" (green bars) if they saw anything. If the subject did not respond within a few seconds after each trial, a response of "No" (red bars) was entered. Turning points (*) were defined as either the second of two consecutive "yes" responses using the same charge per phase during the "up" phase, and the first "no" response during the "down" phase. Threshold (yellow line) was defined as the average charge per phase across the last six turning points (in this case 140nC).

Electrode Configurations and Stimulus Parameters

Stimulus parameters were systematically varied to assess their effects on thresholds. One of six return configurations (Fig. 5) was chosen in decreasing order of the likelihood of current spread: monopolar using one of the 2mm disks as a return; common ground, where the return electrode consisted of all electrodes shorted together except the stimulating electrode; bipolar, where an electrode adjacent to the stimulating electrode was the return; tripolar, where two electrodes adjacent to the stimulating electrode were shorted to form the return; and hexagonal, where five or six electrodes surrounding the active electrode were shorted together as the return. A special case of pseudo-hexagonal was also tested where one of the 2mm disks was shorted to the six electrodes surrounding the stimulating electrode, thus approximating a 50% monopolar and 50% hexagonal situation. In addition, the pulse polarity (cathodic-first or anodic-first, CF or AF), pulse width (PW, up to 500µs per phase), interphase gap (IPG, up to 500µs) and stimulation rate (up to 500pps) were varied.

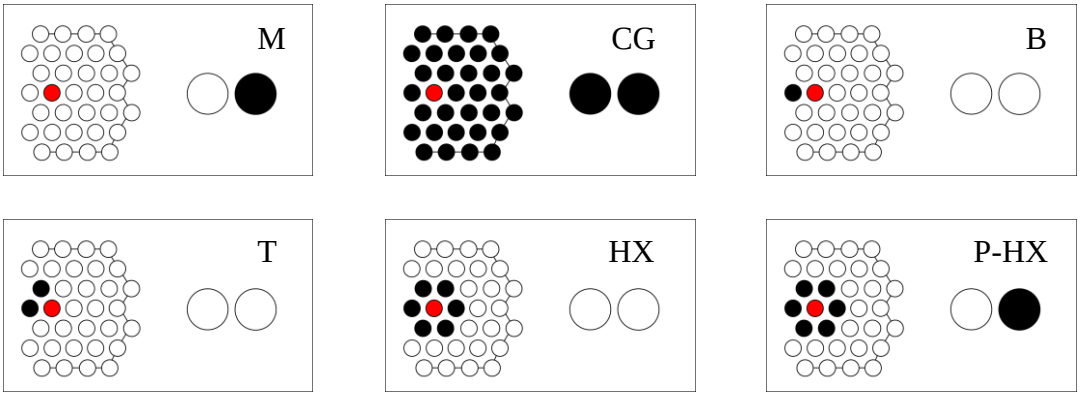

Figure 5. Illustration of the various return configurations tested. In each return configuration shown, the red electrode represents the active stimulating electrode and the black electrodes were shorted together to form the return electrode. M = Monopolar, CG = Common Ground, B = Bipolar, T = Tripolar, HX = Hexagonal, P-HX = Pseudo-Hexagonal.

Statistical Analyses

All thresholds were expressed in nanocoulombs charge per phase per pulse. Statistical analysis was performed in Minitab (State College, PN). The effects of number of days post-implantation, electrode-retina distance and retinal thickness on perceptual thresholds were assessed using linear regression analyses. The effects of all other factors on thresholds were tested using separate general linear models (GLM) with number of days post-implantation designated as a co-variate and the patient number designated as a random factor. Data from P1 and P2 were included in most analyses. Data from P3 were analyzed separately due to previously mentioned issues and the inability to test a large range of stimulus parameters. When assessing the effect of one factor on thresholds, all the other parameters were kept constant. As the distribution of thresholds was found to violate normality (Anderson-Darling test, $p < 0.01$), data were logarithmically transformed before performing GLM and regression analyses. Most data were plotted using box plots, where outliers were defined as threshold

values that were at least 1.5 times above or below the interquartile range (defined as the difference between the third and first quartiles). Outliers were only marked on the plots for display purposes and not removed from the dataset prior to statistical analyses.

Results

Threshold Yield

The threshold yield was defined as the percentage of electrodes where a reliable threshold was reached below the safe charge limit (447nC for 600µm diameter electrodes, 298nC for 400µm diameter electrodes). Table 1 summarizes the efficacy of eliciting phosphenes on individual electrodes and indicates stimulus parameters which were most effective in obtaining a valid threshold. Most data were collected using a stimulation rate of 50pps using a 500µs per phase pulse width and a 500µs interphase gap. Using these parameters, valid thresholds could be obtained on all electrodes tested in P1 using both pulse polarities, with the exception of hexagonal CF stimulation where only 50% of the electrodes tested yielded a threshold within the safe charge limit. When P2 commenced psychophysics sessions, there were some difficulties in obtaining thresholds on 100% of electrodes, even with monopolar stimulation. Moreover, although a valid threshold could be measured with P2 using a stimulation rate of 50pps, he would describe the phosphene as two quick flashes, one appearing at the onset of stimulation and the other appearing at the offset with no percept in between. In addition, the onset and offset flashes were described to be in different locations which made it very confusing for the patient. This led us to explore high rate stimulation with P2. Using high rate stimulation (500pps) with the same pulse width and interphase gap not only made P2's phosphenes appear complete, but also enabled a 100% success rate of valid thresholds. When the pulse width and interphase gap were considerably shortened to 148µs per phase and 20µs respectively, and the rate was slightly decreased to 400pps to allow for sequential stimulation of multiple electrodes during other psychophysical tests (details not included in present manuscript), the yield in P2 was reduced with a valid threshold obtained in 85% of electrodes tested when using AF stimulation (Table 1).

We first began testing high rate stimulation on P3 as it was already shown to be of benefit to P2. Although thresholds could be measured on 12 of 14 single electrodes tested with AF stimulation, the threshold values were found to be very high (>300nC) leaving only ~100nC of headroom below the safe charge limit. In order to alleviate this problem, we switched to testing ganged pairs of adjacent electrodes, where two adjacent electrodes were shorted together as the stimulating active electrode, as opposed to single electrode stimulation. Using ganged pairs increased the maximum safe charge per phase because of the larger total electrode area, thus increasing the available headroom, and the yield compared to stimulation of single electrodes. With stimulation of ganged pairs, we were able to obtain thresholds in P3 with 100% success for the pairs tested, both with 200µs and 500µs per phase pulse widths, 200µs and 500µs interphase gaps, and at stimulation rates of 200pps and 500pps (Table 1).

A total of 565 threshold measurements from P1 (up to 680 days post-implantation), 304 measurements from P2 (up to 619 days post-implantation) and 129 measurements (35 measurements from single electrodes, 94 measurements from ganged pairs) from P3 (up to 539 days post-implantation) were made. Of these, 96.1% of measurements for P1, 89.8% for P2 and 90.7% for P3 (65.7% for single electrode stimulation, 100% for ganged pair stimulation), yielded a threshold value below the safe charge limit. Threshold values for single electrode stimulation ranged from 44-402nC in P1, 53-436nC in P2, and 188-414nC in P3. Threshold values for ganged pair stimulation in P3 ranged from 185-691nC. Based on the yield data for each patient and after working with each one of them for several sessions, a working set of stimulus parameters were established where phosphenes were reliable, thresholds were low, yield was high, and a suitable balance was achieved between PW, IPG and rate to allow for appropriate sequential stimulation of electrodes during other psychophysical tests. More importantly, in each patient, the most threshold data were collected using these working stimulus parameters and thus threshold values could be

monitored over an extended duration, but these parameters were not necessarily the parameters required to obtain the lowest thresholds in each patient. The working stimulus parameters for each patient were determined as;

P1: single electrodes, monopolar, CF, 500µs PW, 500µs IPG, 50pps

P2: single electrodes, monopolar, AF, 148µs PW, 20µs IPG, 400pps

P3: ganged pairs, monopolar, AF, 200µs PW, 200µs IPG, 200pps

		Electrode Threshold Yield		
		P1	**P2**	**P3**
RETURN CONFIGURATION	**Monopolar 500µs PW, 500µs IPG, 50pps**	20/20 (CF) 20/20 (AF)	4/4 (CF) 18/20 (AF)	- (CF) - (AF)
	Common Ground 500µs PW, 500µs IPG, 50pps	19/19 (CF) 19/19 (AF)	2/3 (CF) 18/20 (AF)	- (CF) - (AF)
	Hexagonal 500µs PW, 500µs IPG, 50pps	4/8 (CF) 8/8 (AF)	- (CF) 1/8 (AF)	- (CF) - (AF)
HIGH RATE, LONG PULSES	**Monopolar 500µs PW, 500µs IPG, 500pps**	6/6 (CF) - (AF)	- (CF) 20/20 (AF)	- (CF) 12/14 (AF)
HIGH RATE, SHORT PULSES	**Monopolar 148µs PW, 20µs IPG, 400pps**	- (CF) 20/20 (AF)	2/2 (CF) 17/20 (AF)	- (CF) - (AF)
HIGH RATE GANGED PAIRS	**Monopolar Ganged Pairs 500µs PW, 500µs IPG, 500pps**	- (CF) - (AF)	- (CF) - (AF)	- (CF) 9/9 (AF)
	Monopolar Ganged Pairs 200µs PW, 200µs IPG, 200pps	- (CF) - (AF)	- (CF) - (AF)	- (CF) 21/21 (AF)

Table 1. For each combination of stimulus pulse parameters and in each of the three patients, table shows the number of single electrodes or ganged pairs for which a valid threshold was measured, out of the total number of single electrodes or ganged pairs tested (Note: maximum of 20 possible single electrodes). PW = Pulse Width; IPG = Interphase Gap; CF =

Cathodic-First; AF = Anodic-First. Stimulus duration was fixed at 2secs in all cases. "-" symbol indicates those parameters where no electrodes were tested. Note: For patient 3, the threshold procedure had to be altered to a three-alternative forced choice method (see text for details).

Effect of Number of Days Post-implantation, Electrode-Retina Distance and Retinal Thickness

Figure 6 shows the effect of time after implantation on thresholds (Fig. 6A) and electrode-retina distance (Fig. 6B) in two patients. Both thresholds and corresponding electrode-retina distance were significantly dependent on, and increased with the number of days post-implantation. For P2, absolute thresholds were not only higher than those for P1 but his threshold increases over time occurred at a much faster rate compared to P1 (less than 100nC increase for P1 over almost 700 days versus more than doubled for P2 over approximately 400 days of measurements). Electrode-retina distance increases over time were also higher for P2 and nearly doubled in a span of 3-4 months, compared to P1, in which there was only ~100-150µm increase in just under two years. However, it should be noted that P2 had significant nystagmus, which led to increased difficulty in obtaining high quality OCT scans, and hence a smaller number of data points were available for P2 than for P1. Since both thresholds and electrode-retina distance were found to increase with time, thresholds were found to correlate significantly with electrode-retina distance (Fig. 6C). There was also a significant but negligible correlation between thresholds and retinal thickness in P1 (Fig. 6D). When analyzing the effects of all other parameters on thresholds, the number of days post-implantation was chosen as a co-variate.

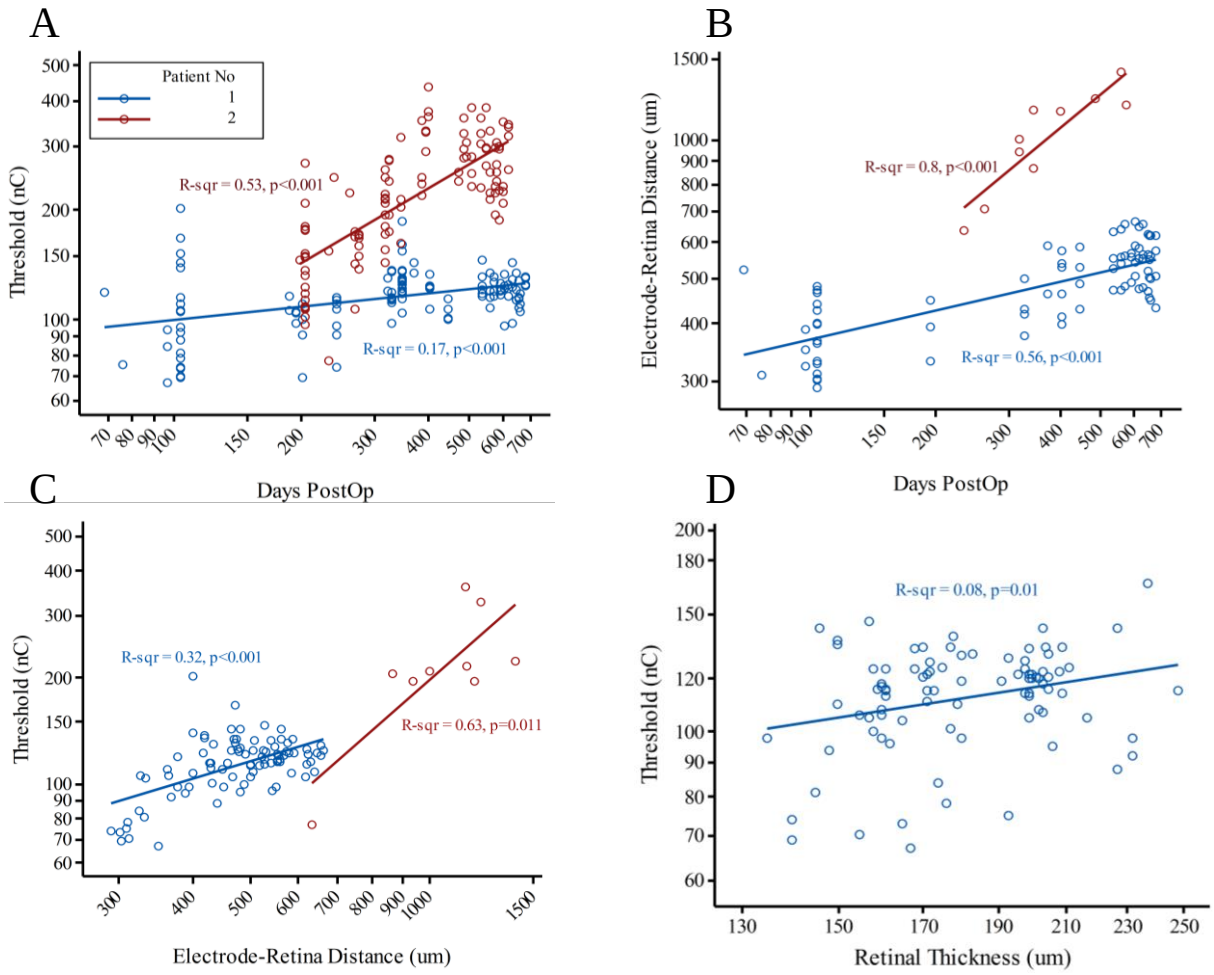

Figure 6. (A & B) Effect of number of days post-implantation on thresholds and corresponding electrode-retina distances. Available data from only those electrodes where thresholds were measured in panel A were included in panel B. (C) Significant correlation between electrode-retina distance and thresholds in P1 and P2. Note: Due to fewer data points available for P2, correlation was not significant. (D) Negligible correlation between retinal thickness and thresholds in P1. Available data from only those electrodes where thresholds were measured in panel A were included in panel C. No retinal thickness data available for P2 due to his nystagmus. For all panels, data were only included for working parameters (P1: 500µs PW, 500µs IPG, 50pps, CF; P2: 148µs PW, 20µs IPG, 400pps, AF). Data are shown on a log-log scale for all panels.

Effect of Electrode Area and Number of Electrodes Stimulated

Surprisingly, thresholds were not dependent on the electrode area or the number of ganged electrodes stimulated. A GLM analysis using data from P1 and P2 (Fig. 7A) showed that thresholds for single electrodes were not dependent on the electrode diameter (400µm, $\bar{x}$ = 124.2nC, n=26 versus 600µm, $\bar{x}$ = 174.2nC, n=211, $p = 0.266$), after accounting for differences due to the number of days post-implantation. Further, while there was a trend of lower thresholds with ganged pairs compared to single electrodes, a separate GLM analysis (Fig. 7B) for P3 revealed that thresholds for single electrodes ($\bar{x}$ = 331.3nC, n=20), were not significantly different ($p = 0.781$) to those for ganged pairs ($\bar{x}$ = 288.7nC, n=27), after accounting for the number of days post-implantation. When further analyzing thresholds for P1 and P2, data from both electrode diameters were pooled together.

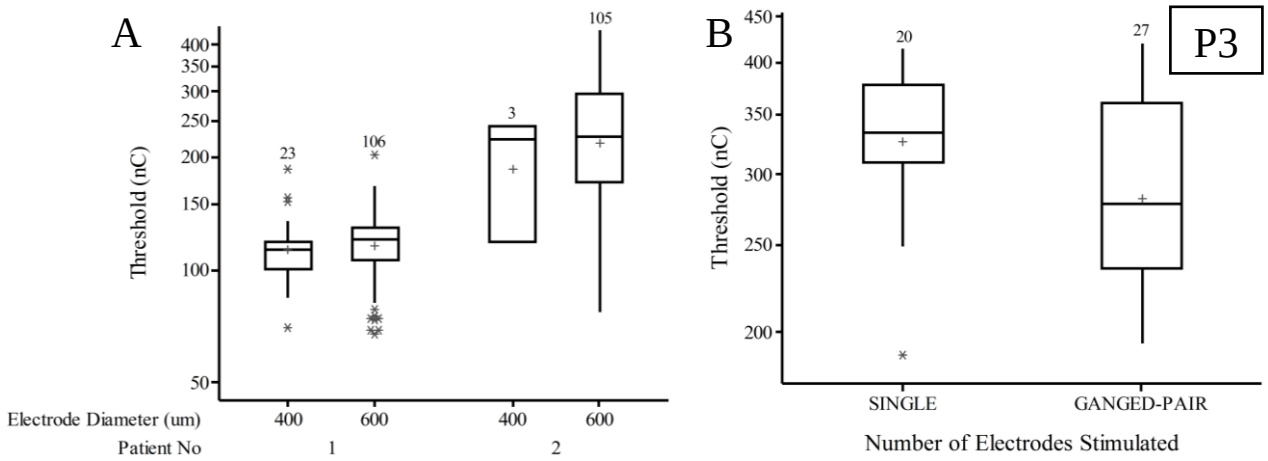

Figure 7. (A) Effect of electrode diameter on thresholds in P1 and P2. Data were included from working parameters (P1: 500µs PW, 500µs IPG, 50pps, CF; P2: 148µs PW, 20µs IPG, 400pps, AF) and from all 20 stimulating electrodes. (B) Effect of retinal area stimulated on thresholds in P3 using either single electrodes or ganged pairs (GP). Pulse parameters were 500µs PW, 500µs IPG, 500pps. For both panels, '+' symbols indicate group means and ''*

symbols indicate outliers. Numbers above whiskers indicate number of data points for each configuration. Note threshold data are plotted on a log axis.

Effect of Return Configuration

As expected, the monopolar return configuration was found to elicit phosphenes with the lowest thresholds regardless of the pulse polarity used, for patients P1 and P2 (Fig. 8). For the same return configuration, thresholds were higher for P2 compared to P1, and generally higher for CF stimulation compared to AF stimulation. Also, in a small number of measurements, changing the monopolar return to the extraocular pin (electrode 24) did not significantly change threshold (data not shown). Compared to monopolar stimulation, thresholds were found to increase when using the common ground configuration, followed by the pseudo-hexagonal, bipolar, tripolar and finally the hexagonal configuration which elicited phosphenes with the highest thresholds. Interestingly, threshold values using the pseudo-hexagonal configuration, (where approximately each half of the current would flow through the monopolar and hexagonal return electrodes) were approximately half-way between those values using the pure monopolar and pure hexagonal configurations. The yield of threshold values being below the safe charge limit also largely depended on the return configuration. A GLM analysis revealed that after accounting for number of days post-implantation and differences between patients, thresholds using the monopolar ($\bar{x}$ = 119.4nC) and common ground ($\bar{x}$ = 151.4nC) configurations were significantly different ($p < 0.001$) to those using all other configurations. The only other significant difference ($p < 0.001$) found was between thresholds using the pseudo-hexagonal configuration ($\bar{x}$ = 206.5nC) and those using the pure hexagonal configuration ($\bar{x}$ = 292.3nC). When further analyzing the effects of other parameters on thresholds, only data using the monopolar configuration were included.

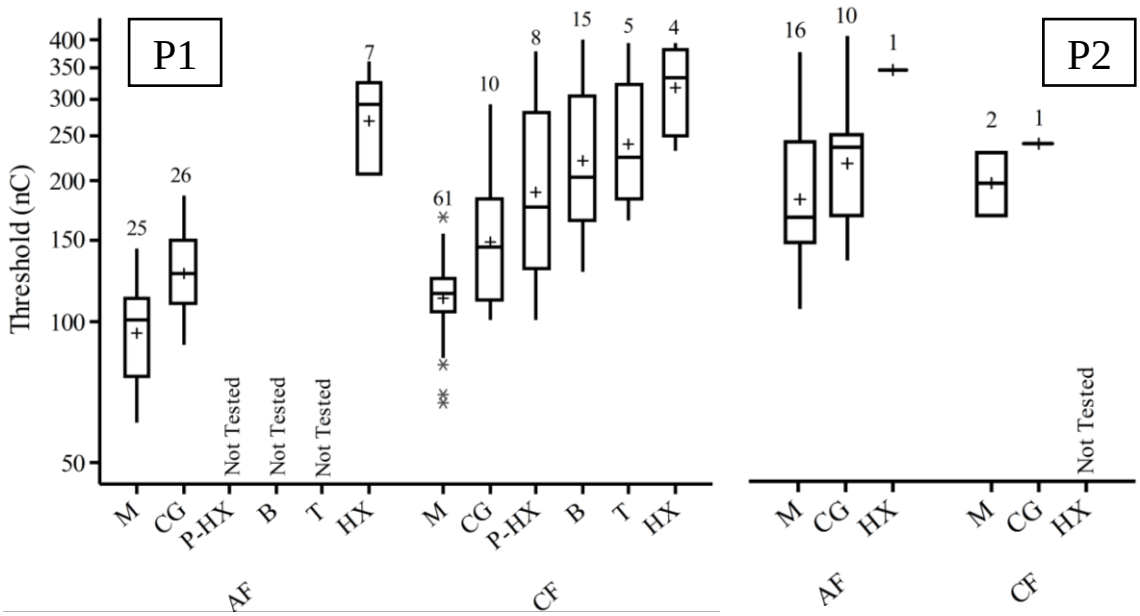

Figure 8. Effect of return configuration on thresholds in P1 and P2. Pulse parameters were fixed at 500µs PW, 500µs IPG, and 50pps rate. '+' symbols indicate group means, '' symbols indicate outliers. Numbers above whiskers indicate number of data points for each configuration. Data is only included from electrodes 2, 7, 12, 3, 8, 13, 4, 9, and 14 (i.e. Electrodes where a hexagonal return would not include the guard ring). Note threshold data are plotted on a log axis.*

Effect of Active Electrode and Pulse Polarity

A GLM analysis was conducted with active electrode and pulse polarity as the factors, number of days post-implantation as the co-variate and patient number as the random factor. There was no significant interaction between active electrode and pulse polarity ($p = 0.765$), while the main effects of both active electrode and pulse polarity were significant ($p < 0.001$). Post-hoc analyses revealed that thresholds using AF stimulation were significantly lower (~20-30nC on average) than those using CF stimulation (Fig. 9).

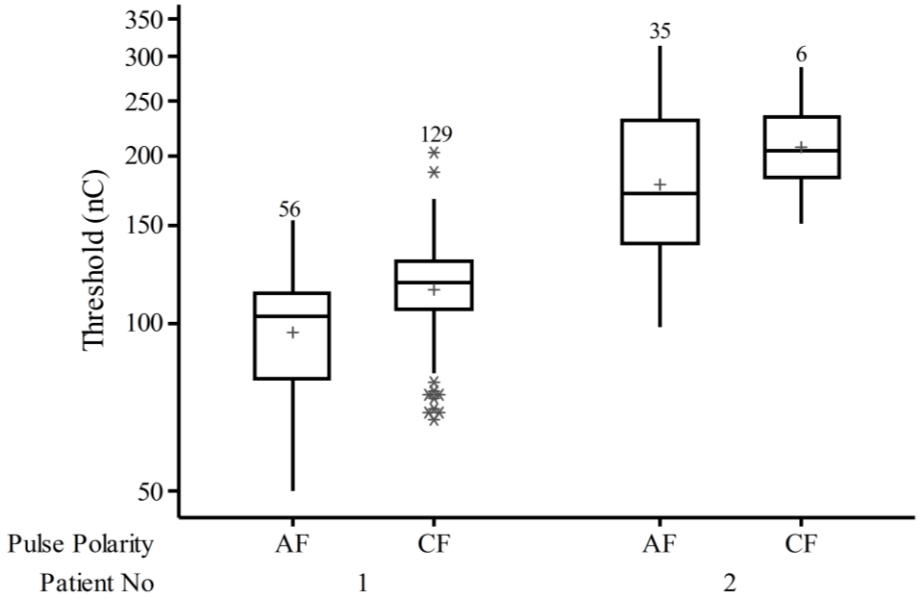

Figure 9. Effect of pulse polarity on thresholds in P1 and P2. Pulse parameters were fixed at 500µs PW, 500µs IPG, 50pps rate. '+' symbols indicate group means, '' symbols indicate outliers. Numbers above whiskers indicate number of data points for each polarity. Data is included from all 20 stimulating electrodes. Note threshold data are plotted on a log axis.*

Effect of Pulse Width and Interphase Gap

Figure 10 summarizes the effects of varying PW and IPG on thresholds in P1 (Fig. 10A) and P2 (Fig. 10B). Generally, larger interphase gaps resulted in lower perceptual thresholds, but this was more evident at shorter values of PW. A GLM analysis with PW and IPG as factors and number of days post-implantation as a co-variate was conducted only for data from P1 as this dataset was more complete. Results showed no significant interaction between PW and IPG ($p = 0.164$). A post-hoc analysis of PW revealed that thresholds using a PW of 100µs per phase ("narrow") were marginally lower (~20nC on average, $p < 0.05$) than those using a PW of 500µs per phase ("wide"). Thresholds using a 200µs per phase PW were not different to narrow or wide pulses ($p > 0.05$). Post-hoc analysis of IPG revealed that only thresholds

using an IPG of 500µs were marginally lower (~20-30nC on average, $p < 0.05$) than those using shorter IPGs (20, 100 and 200µs).

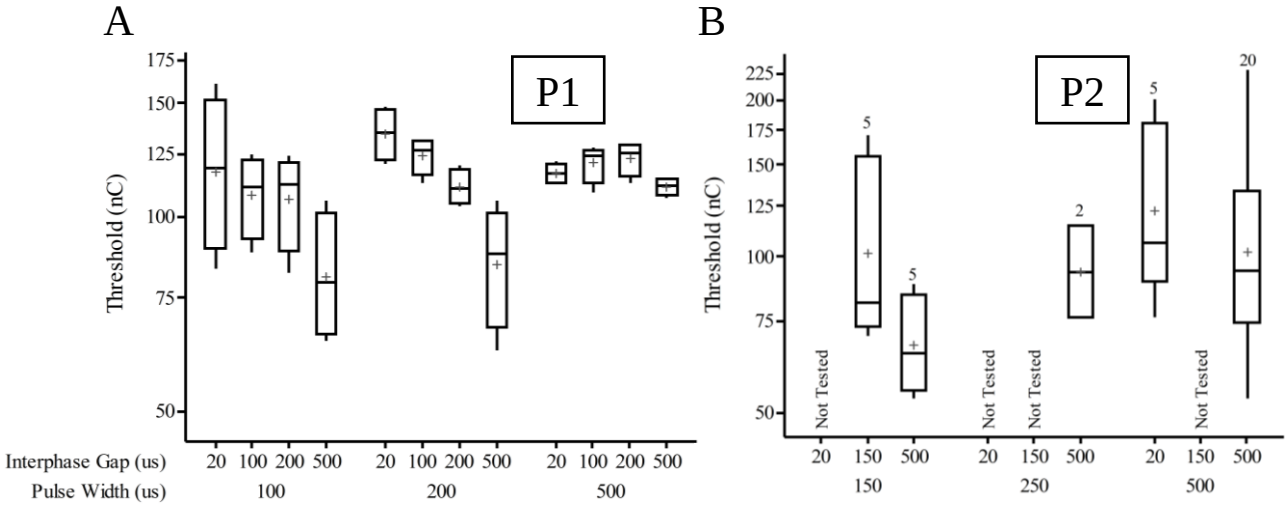

Figure 10. Effect of pulse width and interphase gap on thresholds. (A) Data from P1, pulse parameters were fixed at CF, 50pps rate. Each box contains 4 data points from four electrodes 1, 2, 9 and 10. (B) Data from P2, pulse parameters were fixed at AF, 500pps rate. Numbers above whiskers indicate number of data points for each PW/IPG combination. '+' symbols indicate group means. Note: GLM analysis was only conducted for P1 due to a more complete dataset. Note threshold data are plotted on a log axis.

Effect of Stimulation Rate

Along with the return configuration, stimulation rate was found to have the most significant influence on perceptual thresholds out of all stimulus pulse parameters, with decreasing thresholds as a function of increasing stimulation rate (Fig. 11). In all three patients, the highest rate tested resulted in significantly reduced perceptual thresholds by 34-43% on average compared to a rate of 50pps. Interestingly, in both P1 and P2, there was a trend for

single pulses to induce phosphene percepts with lower thresholds compared to a 5pps pulse train, but this was not significant after accounting for number of days post-implantation.

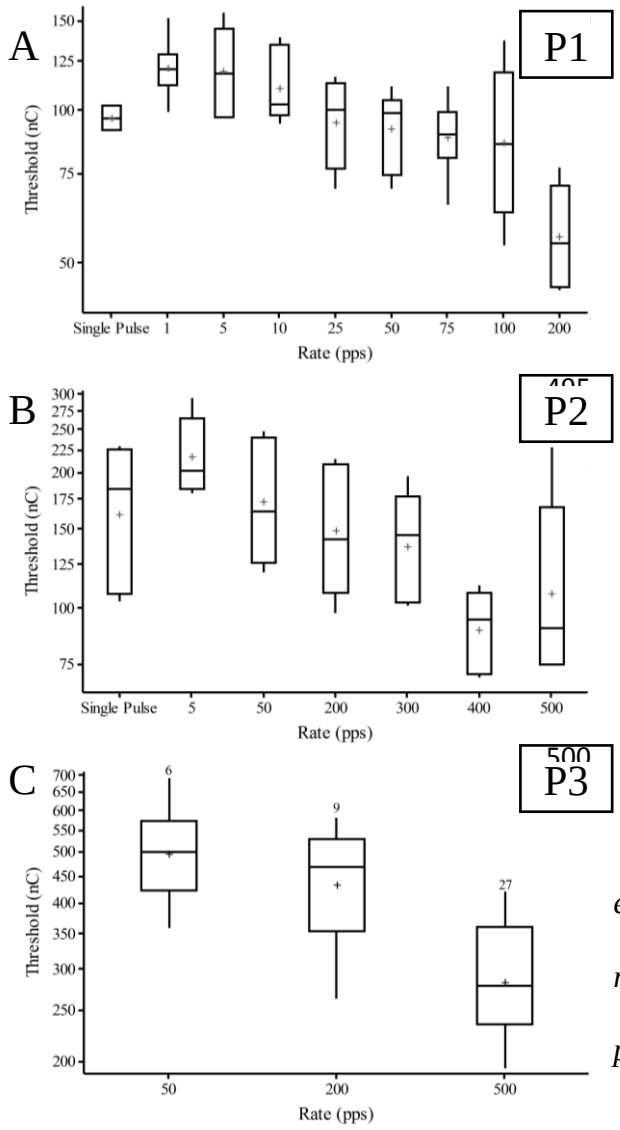

Figure 11. Effect of stimulation rate on perceptual thresholds. (A) Data from P1, pulse parameters were fixed at CF, 500µs PW, 500µs IPG. Each box contains 6 data points from six electrodes 1, 2, 3, 8, 9 and 10. (B) Data from P2, pulse parameters were fixed at AF, 500µs PW, 500µs IPG. Each box contains 5 data points from five electrodes 1, 5, 8, 16, and 20. (C) Data from P3 using ganged pairs, pulse parameters were fixed at AF, 500µs PW, 500µs IPG. Numbers above whiskers indicate number of data points for each rate tested. '+' symbols indicate group means in all panels. Note threshold data are plotted on a log axis.

Discussion

The main goals of this study were to provide evidence of successful stimulation of the retina via an electrode array placed in the suprachoroidal space of profoundly vision impaired humans, assess thresholds required to elicit phosphene percepts, and discover what stimulus parameters and other associated factors affected thresholds the most. Our study monitored thresholds over a duration of just under two years in three patients with profound vision loss from RP. We found that apart from electrode area, the number of ganged electrodes stimulated, and retinal thickness, all factors tested had a significant influence on perceptual thresholds. Charge per phase thresholds were found to be lowest when using anodic-first biphasic pulses with a long interphase gap, in a monopolar return configuration, at high rates of stimulation. Other factors that affected thresholds were the individual patient, active electrode chosen for stimulation, time after implantation, and electrode-retina distance.

Threshold Range and Patient Influence on Thresholds

The perceptual thresholds for single electrodes recorded in this study were ranged widely from as low as 44nC per phase in P1 (Monopolar, CF, 500µs PW, 500µs IPG, 500pps) to as high as 436nC per phase in P2 (Monopolar, AF, 148µs PW, 20µs IPG, 400pps). This type of variability and the large range of thresholds across patients seen in our study has also been seen with epiretinal stimulation[32, 33]. Presumably, the factor likely responsible for the greatest variability amongst patients in our study was the electrode-retina distance (over the duration of the study, electrode-retina distances ranged between 253-780µm in P1, 422-1420µm in P2 and 279-1296µm in P3), but there could be other unknown factors involved, including the density and health of surviving neurons in the retina. Nevertheless, the fact that we were able to obtain thresholds in all 3 patients through careful optimization of stimulus parameters,

provides a proof of concept that suprachoroidal stimulation is a viable option for a retinal prosthesis.

When compared with the thresholds reported for chronic epiretinal stimulation in humans using similar stimulus parameters, the thresholds in our study were found to be higher (Table 1). However, the difference was not as extreme as previously expected, based on an *in vitro* study which showed that suprachoroidal stimulation required ~15 times on average higher charge to reach the threshold of cortical activity compared to subretinal stimulation[34]. When compared to a previous study testing stimulation of the retina via intra-scleral electrodes, thresholds in our study were found to be significantly lower (Table 2).

STUDY	**DURATION & IMPLANT LOCATION**	**STIMULUS PARAMETERS FOR THRESHOLD MEASUREMENTS**	**REPORTED MEAN THRESHOLD**	**PRESENT STUDY CLOSEST MATCHED STIMULUS PARAMETERS**	**PRESENT STUDY MEAN THRESHOLD (600µm electrodes)**
de Balthasar et al[35] (Argus I) – Subjects S4, S5 & S6	CHRONIC EPIRETINAL	Monopolar, 975µs PW, 975µs IPG, Single Pulse, CF	98.87nC & 186.2 µC/cm^2 for 260µm electrodes; 95.87nC & 45.1 µC/cm^2 for 520µm electrodes	Monopolar, 500µs PW, 500µs IPG, Single Pulse, CF (P1), AF (P2)	165.6nC & 58.6µC/cm^2 (n = 11)
Ahuja et al[19] (Argus II)	CHRONIC EPIRETINAL	Monopolar, 450µs PW, 0µs IPG, 20pps, CF	92.925nC & 295.8µC/cm^2 (n = 703)	Monopolar, 500µs PW, 20µs IPG, 50pps, CF	164.2nC & 58.1µC/cm^2 (n = 42)
Fujikado et al[18]	SEMI-CHRONIC SUPRACHOROIDAL-TRANSRETINAL	Monopolar, 500µs PW, 500µs IPG, 20pps, CF	332.5nC & 79.8 µC/cm^2 (n = 10)	Monopolar, 500µs PW, 500µs IPG, 25pps, CF	108.2nC & 38.3 µC/cm^2 (n = 6)
Rizzo et al[32]	ACUTE EPIRETINAL	Monopolar, 250µs PW, 10µs IPG, 20pps, CF	4100µC/cm^2 (100µm) & 300µC/cm^2 (400µm)	Monopolar, 200µs PW, 20µs IPG, 50pps, CF	135nC & 47.8µC/cm^2 (n = 4)
Keseru et al[33]	ACUTE EPIRETINAL	Monopolar, Asymmetric Pulses	Not Comparable		
Klauke et al[36]	SEMI-CHRONIC EPIRETINAL	Interleaved Stimulation of Bipolar Pairs	Not Comparable		

Table 2. Comparison of perceptual thresholds recorded in this study against thresholds recorded in previous retinal prosthesis studies in blind humans. Only similar parameters

used in each study were compared if available. Note, in the comparison with Argus I subjects, direct mean data from S1, S2 and S3 were not available. Also, data from P3 were excluded from the table due to the fact that most data were collected using ganged pair stimulation (which has not been used by any other clinical study) and using different stimulus parameters.

Stimulus Parameter Influence on Thresholds

Effect of Return Configuration:

The influence of return configuration has been well documented in both animal[37-39] and clinical[40-44] studies with cochlear implants. Narrower electric fields in the cochlea using common ground, bipolar and tripolar stimulation result in higher thresholds of either recorded brain activity or perception, and the monopolar return configuration has been shown to produce percepts with the lowest thresholds. An important difference to note between cochlear and retinal implants is the latter makes use of a two-dimensional electrode array as opposed to a linear array, thus allowing one to test even more spatially restricted configurations compared to bipolar and tripolar stimulation. One such configuration we assessed was the hexagonal return, first proposed by Lovell et al[45]. Perceptual thresholds in our study with the hexagonal return were found to be on average 2.5 times higher than those using the monopolar return. In addition to being the first report of hexagonal stimulation in humans, this result is consistent with what has been seen in preclinical retinal implant studies, where between 2 times[23] to 6 times[46, 47] higher thresholds for hexagonal stimulation compared to monopolar stimulation have been reported. Although our preclinical study showed that return configurations such as common ground and hexagonal produce a narrower spread of activation in the retina compared to monopolar stimulation[23], the benefits of using such return configurations for retinal stimulation are at present unclear. Apart from the threshold rise, our

subjects did not report any systematic or significant noticeable effects on phosphene percepts as the return configuration was varied but this was not quantified. Perhaps the benefits of return configurations with spatially restricted fields of excitation will be more evident when performing simultaneous or sequential stimulation of electrodes, where electrode interactions will significantly influence the resultant percept, albeit with the known limitation of requiring 2.5 times higher charge levels. However, there is a possibility that because of the higher current levels required, the group of neurons stimulated by these narrow return configurations may actually be very similar to those when using monopolar stimulation.

Effect of Pulse Polarity:

Clinically, compared to the return configuration, the influence of pulse polarity on perceptual threshold is still debatable. Cochlear implants typically have been shown to produce activation with similar thresholds for CF and AF stimulation, during both electrophysiology[48, 49] and psychophysics testing[48, 50]. However, there are also studies using pulses with long interphase gaps or monophasic pulses, which have shown that anodic currents result in more efficient activation of the cochlea[51-53], but this can also be species dependent[54]. In the retinal implant field, studies by Jensen and Rizzo using subretinal stimulation showed that AF pulses resulted in lower thresholds for activation of RGCs compared to CF pulses[55], but the opposite was true for epiretinal stimulation[56, 57]. Our preclinical study using suprachoroidal stimulation[25] showed that for the same amount of cortical activation, AF stimulation required less charge per phase compared to CF stimulation, which is consistent with the results reported in this study. The most likely explanation for the relatively small benefit seen with AF stimulation in our study, comes from the notion that anodic currents tend to excite neurons that are distal to the stimulating electrode[58], which would most likely be the case with our electrodes being suprachoroidal, and the RGCs being hundreds of microns away.

This notion is further supported by a study that performed recordings in both superficial and deeper layers of the motor cortex in response to electrical stimulation of the cortical surface, where they found neurons in deeper layers to be more sensitive to AF stimuli[59]. Thus clinically, at least for suprachoroidal prostheses, AF stimulation is recommended when using symmetric biphasic pulses.

Effect of Pulse Width, Interphase Gap and Stimulation Rate:

Our study showed a marked reduction in perceptual threshold when using short-duration pulse widths combined with long interphase gaps compared to other pulse width-interphase gap combinations. While this result is well established in the cochlear implant literature[60, 61], recent reports with epiretinal stimulation[62, 63] and our preclinical study using suprachoroidal stimulation[25] have also demonstrated the beneficial effects of using an interphase gap with biphasic pulses compared to pulses without any interphase gap. In fact, the study by Weitz et al[63] showed an improvement of ~10% in perceptual threshold when using interphase gaps of ≥ 500µs compared to no gap with the pulse width set to 450µs per phase, a result very closely matched with what we found when using a PW of 500µs per phase. The effect of PW alone on threshold is also well established, where longer PWs have been shown to increase threshold charge per phase and decrease threshold current (strength-duration curve), both with cochlear implants[64] and retinal implants[25, 32]. In our study, although we only tested a limited number of PW and IPG combinations due to time constraints, our data support the present literature.

While the benefit of high stimulation rates on perceptual threshold is well known with cochlear implants[20, 65, 66], it has not been extensively reported in humans with retinal stimulation. A study by Horsager et al[21] showed some promise for high rate epiretinal stimulation, with significantly reduced threshold currents for rates up to 135pps using long

duration pulse trains, and up to 3,000pps using short duration pulse trains. However, when their data were converted to total charge delivered over a 500ms pulse train and fitted using their model, they predicted that high stimulation rates required more total charge to reach threshold for a given PW. These results led to their conclusion that the most effective rate for epiretinal stimulation is 50pps. It is likely that the duration of stimulation will govern the most effective stimulus rate in terms of lower total charge delivered due to differences in the number of pulses. At longer durations, a 50pps pulse train may require less total charge compared to a 400pps pulse train, however for short duration stimulation (more likely to occur when using a camera-based strategy), a higher rate will be preferential as the charge per pulse is significantly reduced.

A problem to consider with high rate stimulation is the possibility of phosphene fading, occurring mostly within a few seconds after stimulation onset, but sometimes much quicker. There have been reports with both epiretinal[67] and subretinal[68] stimulation, that higher stimulation rates cause faster fading than lower rates, but the opposite can also be true, so the data are not consistent across subjects[67]. However, the typical rates used to test phosphene fading have only been up to tens of pps as opposed to hundreds of pps that we tested. Our patients reported no major fading of phosphenes and were able to see the phosphene for the total duration of stimulation (2 secs in this study), but we did not systematically quantify the effects of fading. P3 was an exception, who only saw a quick flash at the onset of stimulation, but this was not stimulus or electrode dependent.

There are two mechanisms which may be responsible for the lower thresholds seen when using high rates. There have been several in-vitro studies using epiretinal and subretinal stimulation, showing that most types of RGCs are typically “desensitized” at high stimulation rates (beyond 200pps) where they may fail to “follow” each pulse within a high rate pulse train, or produce no spiking at all[69-71]. However, there are some types of RGCs that can even

follow 600pps stimulation[72], and a recent study performing epiretinal stimulation showed robust responses in ON-OFF directionally sensitive RGCs when stimulation was applied at 2000pps[73]. It is possible that higher rates may provide exclusive activation of RGCs as opposed to the remaining neural network, thus bringing down thresholds and eliciting clearer phosphenes. Alternatively, the reason for high rate stimulation to work well could simply be a central mechanism, where integration of multiple pulses within a short temporal window could significantly increase detectability of the stimulus, a feature prominent in both the visual[74] and auditory[75] systems.

Ultimately, the decision to use high rates will be partly governed by the threshold charge level required, electrode impedances and voltage and current limitations of the stimulator. High rates will likely require short PWs for sequential stimulation of multiple electrodes and therefore, large currents and voltages to evoke percepts. In addition, one must bear in mind that the prosthesis in normal operation is expected to be stimulating at levels of up to 1.5-2 times above threshold, so the stimulator design would need to supply large currents and voltages, a challenge when using miniature components. In such situations, perhaps a low stimulation rate with long pulses would be more suitable.

Influence of Other Factors on Thresholds

Apart from stimulus parameters, we found that thresholds depended significantly on electrode-retina distance but negligibly on retinal thickness. A study using the Argus I epiretinal prosthesis also found that retinal thickness was not a determinant factor of threshold[35]. One reason for the weak correlation could be that while visual acuity in RP patients depends on the preservation of macular photoreceptors, the level of preservation may not be proportional to the overall retinal thickness, as it has been shown that visual acuity and foveal retinal thickness do not correlate in all RP patients[76]. Also, the macular volume does

not highly correlate with remaining residual function in a degenerate retina[77], so in some ways one might expect no correlation between retinal thickness and threshold. Furthermore, the Argus I study found that electrode-retina distance was a significant determinant of threshold, similar to the findings of this study. Interestingly, in our study the electrode-retina distance was highly variable, not only across patients but even amongst electrodes within each patient. Therefore, it is also possible that the high variability in electrode-retina distance across the electrode array was responsible for the weak correlation between threshold and the retinal thickness directly above each electrode due to confounding measurements between electrode-retina distance and retinal thickness. The variability seen within each patient was partly attributed to limitations with the measurement tool on the OCT equipment and partly due to the location of the electrodes on the array. Measurement error could easily be 10-20µm, and this would lead to fluctuations in measurement values. In addition, the electrodes on the outer edge of the array always tended to be closer to the retina, as the area of presumed fibrosis overlying the array was thickest in the middle, causing more elevation of the retina compared to the edges. However, there was a clear trend for increasing electrode to retina distance with time, despite these limitations.

The electrode diameter or the number of ganged electrodes stimulated also did not affect thresholds, seen when comparing thresholds from single electrodes (two different electrode diameters) in P1 and P2, and when comparing single electrodes versus ganged pairs (600µm diameter only) in P3. The finding related to electrode area is consistent with what we have previously reported in a preclinical study measuring evoked potential thresholds[78], and is also consistent with findings from patients with epiretinal implants[35]. While larger electrodes may be expected to result in higher thresholds[70], it is possible that the 600µm diameter electrodes in our study have more uneven current distribution across the electrode surface compared to the 400µm diameter electrodes, with more current density around the edges, thus accounting

for similar thresholds[35]. It must be noted however, that the only way to change the electrode diameter was to change the active electrode on the array being stimulated, therefore electrode diameter and electrode location always co-varied. Therefore, it is also possible that we were not able to isolate the effects of electrode diameter alone on threshold. The second finding may be a little surprising at first, as one may expect a larger retinal area covered by two ganged 600µm electrodes to elicit a lower perceptual threshold than a single electrode if one assumes the higher probability of exciting more neurons with ganged-pair stimulation. However, if edge effects of current distribution play a role, then ganging two electrodes may not have the same effect as increasing the area of retina being stimulated. When taking into account the above two findings, it may be beneficial for a suprachoroidal retinal prosthesis to use larger diameter electrodes as opposed to smaller electrodes to take advantage of the significantly lower impedances and lower charge densities that larger electrodes offer. Also, as learnt from the experience with P3, ganged pairs of electrodes can be used as a fallback in case single electrode stimulation is unable to elicit phosphenes, since the effects of stimulus parameters on thresholds are likely to be similar with both single electrode and ganged pair stimulation.

The increase in thresholds over time is of some concern. With the Argus I prosthesis, thresholds also increased with time, and this was suggested to be a result of the electrode lifting off the retina after surgery, thus increasing the electrode-retina distance[35]. It is well known that threshold is strongly correlated with electrode-retina distance, both *in vitro* and *in vivo*. In our study, we also observed an increase in electrode-retina distances over time, and therefore this may explain the increase in threshold over time. At this stage, it is unclear as to what exactly caused the longitudinal increase in electrode-retina distances, and this is currently under further investigation. Many factors could be responsible but it is likely to be associated with the formation of fibrous tissue around the array. The rate of increase varied

between patients, which may be related to the time taken for the initial hemorrhage to resolve in each patient or the level of nystagmus. For example, P2 had the largest electrode-retina distances and the most severe nystagmus, while P1 had almost no nystagmus and the smallest change in distance. The rate of fibrous growth could also have possibly depended on stimulus levels used (P2 and P3 had higher thresholds compared to P1). Studies are currently being conducted to identify the exact cause of the increase observed, but it highlights the need to carefully monitor electrode-retina distances over the long-term when using suprachoroidal stimulation, as this is likely to be an important factor governing the success of this implant.

Conclusion

Our study is the first of its kind to report the factors affecting perceptual thresholds with suprachoroidal stimulation over long-term implantation. Firstly, we showed that through careful optimization of stimulus parameters, it was possible to obtain reliable thresholds and phosphene percepts in all three patients, thus proving that suprachoroidal stimulation can be effective. Secondly, we showed that for suprachoroidal stimulation, using the monopolar return configuration and AF polarity, along with short pulse widths combined with long interphase gaps and high stimulation rates, we can maximally reduce perceptual thresholds. Lastly, future investigations will need to carefully monitor electrode-retina distances and attempt to elucidate the cause of increasing thresholds over time.

References

1. Brindley GS, Lewin WS. The sensations produced by electrical stimulation of the visual cortex. *J Physiol*. 1968;196:479-493.

2. Brindley GS, Lewin WS. The visual sensations produced by electrical stimulation of the medial occipital cortex. *J Physiol*. 1968;194:54-55P.

3. Stronks HC, Dagnelie G. The functional performance of the argus ii retinal prosthesis. *Expert Rev Med Devices*. 2013;11:23-30.

4. Stingl K, Bartz-Schmidt KU, Besch D et al. Artificial vision with wirelessly powered subretinal electronic implant alpha-ims. *Proc Biol Sci*. 2013;280:20130077.

5. Humayun MS, da Cruz L, Dagnelie G et al. Results update from second sight's argus(r) ii retinal prosthesis study. *ARVO Meeting Abstracts*. 2012;53:6953.

6. daCruz L, Merlini F, Arsiero M et al. Subjects blinded by outer retinal dystrophies are able to recognize outlined shapes using the argus(r) ii retinal prosthesis system: A comparison with the full shapes recognition task. *ARVO Meeting Abstracts*. 2012;53:5507.

7. Dorn JD, Ahuja AK, Caspi A et al. The detection of motion by blind subjects with the epiretinal 60-electrode (argus ii) retinal prosthesis. *Arch Ophthalmol*. 2012:1-7.

8. Stingl K, Bartz-Schmidt KU, Gekeler F, Kusnyerik A, Sachs H, Zrenner E. Functional outcome in subretinal electronic implants depends on foveal eccentricity. *Invest Ophthalmol Vis Sci*. 2013;54:7658-7665.

9. Stingl K, Bartz-Schmidt KU, Besch D et al. [what can blind patients see in daily life with the subretinal alpha ims implant? Current overview from the clinical trial in tubingen]. *Ophthalmologe*. 2012;109:136-141.

10. da Cruz L, Coley BF, Dorn J et al. The argus ii epiretinal prosthesis system allows letter and word reading and long-term function in patients with profound vision loss. *Br J Ophthalmol*. 2013;97:632-636.

11. Stingl K, Gekeler F, Bartz-Schmidt KU, Kogel A, Zrenner E, Gelisken F. Fluorescein angiographic findings in eyes of patients with a subretinal electronic implant. *Curr Eye Res*. 2013;38:588-596.

12. Stanga PE, Hafezi F, Sahel JA et al. Patients blinded by outer retinal dystrophies are able to perceive color using the argustm ii retinal prosthesis system. *ARVO Meeting Abstracts*. 2011;52:4949.

13. Gekeler F, Szurman P, Besch D et al. Implantation and explantation of active subretinal visual prostheses using a combined transcutaneous and transchoroidal approach. *Nova Acta Leopoldina NF 111*. 2010;379:205-216.

14. Stingl K, Bach M, Bartz-Schmidt KU et al. Safety and efficacy of subretinal visual implants in humans: Methodological aspects. *Clin Exp Optom*. 2013;96:4-13.

15. Saunders AL, Williams CE, Heriot W et al. Development of a surgical procedure for implantation of a prototype suprachoroidal retinal prosthesis. *Clin Experiment Ophthalmol*. 2013.

16. Villalobos J, Nayagam DAX, Allen PJ et al. A wide-field suprachoroidal retinal prosthesis is stable and well tolerated following chronic implantation. *Invest Ophthalmol Vis Sci*. 2013:In Press.

17. Shepherd RK, Shivdasani MN, Nayagam DA, Williams CE, Blamey PJ. Visual prostheses for the blind. *Trends Biotechnol*. 2013;31:562-571.

18. Fujikado T, Kamei M, Sakaguchi H et al. Testing of semichronically implanted retinal prosthesis by suprachoroidal-transretinal stimulation in patients with retinitis pigmentosa. *Invest Ophthalmol Vis Sci*. 2011;52:4726-4733.

19. Ahuja AK, Yeoh J, Dorn JD et al. Factors affecting perceptual threshold in argus ii retinal prosthesis subjects. *Transl Vis Sci Technol*. 2013;2:1.

20. Zhou N, Xu L, Pfingst BE. Characteristics of detection thresholds and maximum comfortable loudness levels as a function of pulse rate in human cochlear implant users. *Hear Res*. 2012;284:25-32.

21. Horsager A, Greenwald SH, Weiland JD et al. Predicting visual sensitivity in retinal prosthesis patients. *Invest Ophthalmol Vis Sci*. 2009;50:1483-1491.

22. Nayagam D, Williams R, Shivdasani M et al. Chronic electrical stimulation of the retina via suprachoroidal electrodes is safe. *ARVO Meeting Abstracts*. 2013;54:1053.

23. Cicione R, Shivdasani MN, Fallon JB et al. Visual cortex responses to suprachoroidal electrical stimulation of the retina: Effects of electrode return configuration. *J Neural Eng*. 2012;9:036009.

24. Shivdasani MN, Fallon JB, Luu CD et al. Visual cortex responses to single- and simultaneous multiple-electrode stimulation of the retina: Implications for retinal prostheses. *Invest Ophthalmol Vis Sci*. 2012;53:6291-6300.

25. John SE, Shivdasani MN, Williams CE et al. Suprachoroidal electrical stimulation: Effects of stimulus pulse parameters on visual cortical responses. *J Neural Eng*. 2013;10:056011.

26. Blamey P, Sinclair N, Slater K et al. Psychophysics of a suprachoroidal retinal prosthesis. *ARVO Meeting Abstracts*. 2013;54:1044.

27. Allen P, Yeoh J, McCombe M et al. Bionic vision australia - implantation of a suprachoroidal retinal prosthesis- results for the first participants. *ARVO Meeting Abstracts*. 2013;54:1031.

28. Ayton LN, Apollo NV, Varsamidis M, Dimitrov PN, Guymer RH, Luu CD. Assessing residual visual function in severe vision loss. *Invest Ophthalmol Vis Sci*. 2014;55:1332-1338.

29. Merrill DR, Bikson M, Jefferys JG. Electrical stimulation of excitable tissue: Design of efficacious and safe protocols. *J Neurosci Methods*. 2005;141:171-198.

30. Shannon RV. A model of safe levels for electrical stimulation. *IEEE Trans Biomed Eng*. 1992;39:424-426.

31. Treutwein B. Adaptive psychophysical procedures. *Vision Res*. 1995;35:2503-2522.

32. Rizzo JF, 3rd, Wyatt J, Loewenstein J, Kelly S, Shire D. Methods and perceptual thresholds for short-term electrical stimulation of human retina with microelectrode arrays. *Invest Ophthalmol Vis Sci*. 2003;44:5355-5361.

33. Keseru M, Feucht M, Bornfeld N et al. Acute electrical stimulation of the human retina with an epiretinal electrode array. *Acta Ophthalmol*. 2012;90:e1-8.

34. Yamauchi Y, Franco LM, Jackson DJ et al. Comparison of electrically evoked cortical potential thresholds generated with subretinal or suprachoroidal placement of a microelectrode array in the rabbit. *J Neural Eng*. 2005;2:S48-56.

35. de Balthasar C, Patel S, Roy A et al. Factors affecting perceptual thresholds in epiretinal prostheses. *Invest Ophthalmol Vis Sci*. 2008;49:2303-2314.

36. Klauke S, Goertz M, Rein S et al. Stimulation with a wireless intraocular epiretinal implant elicits visual percepts in blind humans: Results from stimulation tests during the epiret3 prospective clinical trial. *Invest Ophthalmol Vis Sci*. 2011.

37. Bierer JA, Middlebrooks JC. Auditory cortical images of cochlear-implant stimuli: Dependence on electrode configuration. *J Neurophysiol*. 2002;87:478-492.

38. Morris DJ, Pfingst BE. Effects of electrode configuration and stimulus level on rate and level discrimination with cochlear implants. *J Assoc Res Otolaryngol*. 2000;1:211-223.

39. Snyder RL, Middlebrooks JC, Bonham BH. Cochlear implant electrode configuration effects on activation threshold and tonotopic selectivity. *Hear Res*. 2008;235:23-38.

40. Busby PA, Whitford LA, Blamey PJ, Richardson LM, Clark GM. Pitch perception for different modes of stimulation using the cochlear multiple-electrode prosthesis. *J Acoust Soc Am*. 1994;95:2658-2669.

41. Pfingst BE, Miller AL, Morris DJ, Zwolan TA, Spelman FA, Clopton BM. Effects of electrical current configuration on stimulus detection. *Ann Otol Rhinol Laryngol Suppl*. 1995;166:127-131.

42. Pfingst BE, Morris DJ, Miller AL. Effects of electrode configuration on threshold functions for electrical stimulation of the cochlea. *Hear Res*. 1995;85:76-84.

43. Pfingst BE, Zwolan TA, Holloway LA. Effects of stimulus configuration on psychophysical operating levels and on speech recognition with cochlear implants. *Hear Res*. 1997;112:247-260.

44. Bierer JA. Threshold and channel interaction in cochlear implant users: Evaluation of the tripolar electrode configuration. *J Acoust Soc Am*. 2007;121:1642-1653.

45. Lovell NH, Dokos S, Preston P et al. A retinal neuroprosthesis design based on simultaneous current injection. In: 3rd Annual International IEEE EMBS Special Topic Conference on Microtechnologies in Medicine and Biology; 2005; Hawaii, USA, 2005: 98-101.

46. Wong YT, Chen SC, Seo JM, Morley JW, Lovell NH, Suaning GJ. Focal activation of the feline retina via a suprachoroidal electrode array. *Vision Res*. 2009.

47. Gerhardt M, Groeger G, Maccarthy N. Monopolar vs. Bipolar subretinal stimulation-an in vitro study. *J Neurosci Methods*. 2011;199:26-34.

48. Bahmer A, Baumann U. Effects of electrical pulse polarity shape on intra cochlear neural responses in humans: Triphasic pulses with cathodic second phase. *Hear Res*. 2013;306:123-130.

49. Shepherd RK, Javel E. Electrical stimulation of the auditory nerve: Ii. Effect of stimulus waveshape on single fibre response properties. *Hear Res*. 1999;130:171-188.

50. Coste RL, Pfingst BE. Stimulus features affecting psychophysical detection thresholds for electrical stimulation of the cochlea. Iii. Pulse polarity. *J Acoust Soc Am*. 1996;99:3099-3108.

51. van Wieringen A, Macherey O, Carlyon RP, Deeks JM, Wouters J. Alternative pulse shapes in electrical hearing. *Hear Res*. 2008;242:154-163.

52. Macherey O, Carlyon RP, van Wieringen A, Deeks JM, Wouters J. Higher sensitivity of human auditory nerve fibers to positive electrical currents. *J Assoc Res Otolaryngol*. 2008;9:241-251.

53. Undurraga JA, van Wieringen A, Carlyon RP, Macherey O, Wouters J. Polarity effects on neural responses of the electrically stimulated auditory nerve at different cochlear sites. *Hear Res*. 2010;269:146-161.

54. Miller CA, Abbas PJ, Rubinstein JT, Robinson BK, Matsuoka AJ, Woodworth G. Electrically evoked compound action potentials of guinea pig and cat: Responses to monopolar, monophasic stimulation. *Hear Res*. 1998;119:142-154.

55. Jensen RJ, Rizzo JF, 3rd. Thresholds for activation of rabbit retinal ganglion cells with a subretinal electrode. *Exp Eye Res*. 2006;83:367-373.

56. Jensen RJ, Rizzo JF, 3rd, Ziv OR, Grumet A, Wyatt J. Thresholds for activation of rabbit retinal ganglion cells with an ultrafine, extracellular microelectrode. *Invest Ophthalmol Vis Sci*. 2003;44:3533-3543.

57. Jensen RJ, Ziv OR, Rizzo JF. Responses of rabbit retinal ganglion cells to electrical stimulation with an epiretinal electrode. *J Neural Eng*. 2005;2:S16-21.

58. Ranck JB, Jr. Which elements are excited in electrical stimulation of mammalian central nervous system: A review. *Brain Res*. 1975;98:417-440.

59. Yazdan-Shahmorad A, Kipke DR, Lehmkuhle MJ. Polarity of cortical electrical stimulation differentially affects neuronal activity of deep and superficial layers of rat motor cortex. *Brain Stimul*. 2011;4:228-241.

60. Carlyon RP, van Wieringen A, Deeks JM, Long CJ, Lyzenga J, Wouters J. Effect of inter-phase gap on the sensitivity of cochlear implant users to electrical stimulation. *Hear Res*. 2005;205:210-224.

61. McKay CM, Henshall KR. The perceptual effects of interphase gap duration in cochlear implant stimulation. *Hear Res*. 2003;181:94-99.

62. Weitz AC, Behrend MR, Humayun MS, Chow RH, Weiland JD. Interphase gap decreases electrical stimulation threshold of retinal ganglion cells. *Conf Proc IEEE Eng Med Biol Soc*. 2011;2011:6725-6728.

63. Weitz AC, Behrend MR, Ahuja AK et al. Interphase gap as a means to reduce electrical stimulation thresholds for epiretinal prostheses. *J Neural Eng*. 2014;11:016007.

64. Moon AK, Zwolan TA, Pfingst BE. Effects of phase duration on detection of electrical stimulation of the human cochlea. *Hear Res*. 1993;67:166-178.

65. McKay CM, Lim HH, Lenarz T. Temporal processing in the auditory system: Insights from cochlear and auditory midbrain implantees. *J Assoc Res Otolaryngol*. 2013;14:103-124.

66. Skinner MW, Holden LK, Holden TA, Demorest ME. Effect of stimulation rate on cochlear implant recipients' thresholds and maximum acceptable loudness levels. *J Am Acad Audiol*. 2000;11:203-213.

67. Perez Fornos A, Sommerhalder J, da Cruz L et al. Temporal properties of visual perception on electrical stimulation of the retina. *Invest Ophthalmol Vis Sci*. 2012;53:2720-2731.

68. Zrenner E, Bartz-Schmidt KU, Benav H et al. Subretinal electronic chips allow blind patients to read letters and combine them to words. *Proc Biol Sci*. 2011;278:1489-1497.

69. Fried SI, Hsueh HA, Werblin FS. A method for generating precise temporal patterns of retinal spiking using prosthetic stimulation. *J Neurophysiol*. 2006;95:970-978.

70. Sekirnjak C, Hottowy P, Sher A, Dabrowski W, Litke AM, Chichilnisky EJ. Electrical stimulation of mammalian retinal ganglion cells with multielectrode arrays. *J Neurophysiol*. 2006;95:3311-3327.

71. Tsai D, Morley JW, Suaning GJ, Lovell NH. Direct activation and temporal response properties of rabbit retinal ganglion cells following subretinal stimulation. *J Neurophysiol*. 2009;102:2982-2993.

72. Cai C, Ren Q, Desai NJ, Rizzo JF, 3rd, Fried SI. Response variability to high rates of electric stimulation in retinal ganglion cells. *J Neurophysiol*. 2011;106:153-162.

73. Cai C, Twyford P, Fried S. The response of retinal neurons to high-frequency stimulation. *J Neural Eng*. 2013;10:036009.

74. Watson AB. Temporal sensitivity. In: Boff K, Kaufman L, Thomas J, eds. Handbook of perception and human performance. New York: Wiley, 1986: 1-43.

75. Gerken GM, Bhat VK, Hutchison-Clutter M. Auditory temporal integration and the power function model. *J Acoust Soc Am*. 1990;88:767-778.

76. Moschos MM, Chatziralli IP, Verriopoulos G, Triglianos A, Ladas DS, Brouzas D. Correlation between optical coherence tomography and multifocal electroretinogram findings with visual acuity in retinitis pigmentosa. *Clin Ophthalmol*. 2013;7:2073-2078.

77. Sugita T, Kondo M, Piao CH, Ito Y, Terasaki H. Correlation between macular volume and focal macular electroretinogram in patients with retinitis pigmentosa. *Invest Ophthalmol Vis Sci*. 2008;49:3551-3558.

78. Shivdasani MN, Luu CD, Cicione R et al. Evaluation of stimulus parameters and electrode geometry for an effective suprachoroidal retinal prosthesis. *J Neural Eng*. 2010;7:036008.